

# Microscopic structure of electrowetting-driven transitions on superhydrophobic surfaces

A. Staicu,\* G. Manukyan, and F. Mugele

*Physics of Complex Fluids, Faculty of Science and Technology,  
University of Twente, PO Box 217,  
7500AE Enschede, The Netherlands*

(Dated: October 25, 2018)

## Abstract

We investigate directly at the microscale the morphology of the electrowetting induced transition between the Cassie-Baxter and Wenzel states for a water droplet on a superhydrophobic surface. Our experiments demonstrate that the transition originates in a very narrow annular region near the macroscopic contact line, which is first invaded by water and causes a thin film of air to be entrapped below. At high applied voltages, a growing fraction of microscopic air-pockets collapse, resulting in a partial Wenzel state. Modulations in the intensity of the light reflected from individual micro-menisci clarify that the local contact angles near the filling transition are close to the usual advancing values for contact lines on smooth surfaces.

It is well known that the presence of roughness at microscale, whether naturally occurring or artificially created, leads to the phenomenon of superhydrophobicity [1]. Depending on whether or not the liquid fills the crevasses of the microscopic texture (typically microscopic pillars uniformly spaced), the mobility of water droplets on such surfaces can be either severely decreased, resulting in sticking drops (Wenzel state[2]) or, respectively, greatly enhanced (Cassie-Baxter state[3]). Effective control of water wettability on smooth surfaces has been demonstrated in material research already for a long time (by external action on droplets by electric fields, light, temperature and chemistry), but only recently these effects have been combined with textured superhydrophobic surfaces in order to drive the transition between the Cassie-Baxter, or air-pocket state, and Wenzel state, when liquid fills the space between the micro-pillars (Fig.1). A situation of considerable interest for industrial applications would be to be able to quickly and reversibly switch between these wetting states in a non-intrusive manner. Recent promising efforts focus on the use of the electrowetting effect (EW). Several studies [4, 5, 6, 7, 8, 9]) reported EW induced transitions from highly mobile droplets to pinned states on microstructured surfaces. These were signaled by more or less abrupt jumps in the observed value of the macroscopic contact angle, which in the

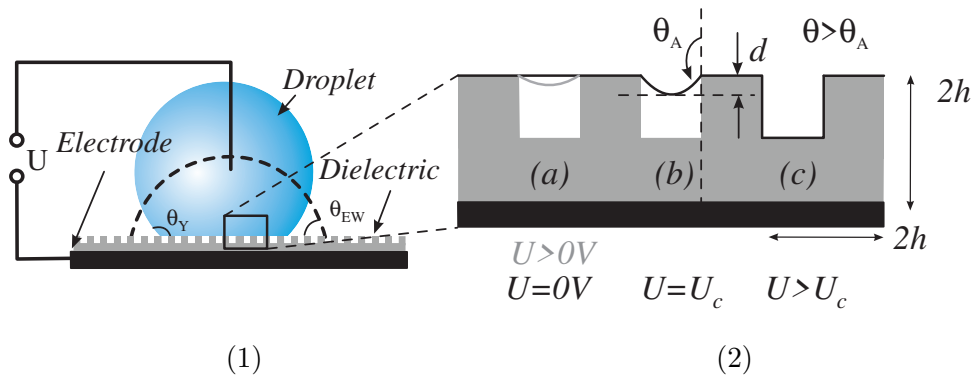


FIG. 1: (1) Electrowetting: a voltage  $U$  is applied between a droplet and an electrode covered with a dielectric micro-patterned surface. The contact area is viewed with an inverted microscope through the superhydrophobic substrate. (2) Scenario for the filling with water of individual micro-pits: (a)  $U = 0$  water menisci are flat and become increasingly curved for  $0 < U < U_c$  (critical voltage); (b) for  $U_c$  such that the contact angle at the vertical walls is the advancing angle  $\approx \theta_A$  the filling process starts; (c) for  $U > U_c$  the menisci advance to the Wenzel state, provided the opposing hydrostatic pressure does not change.

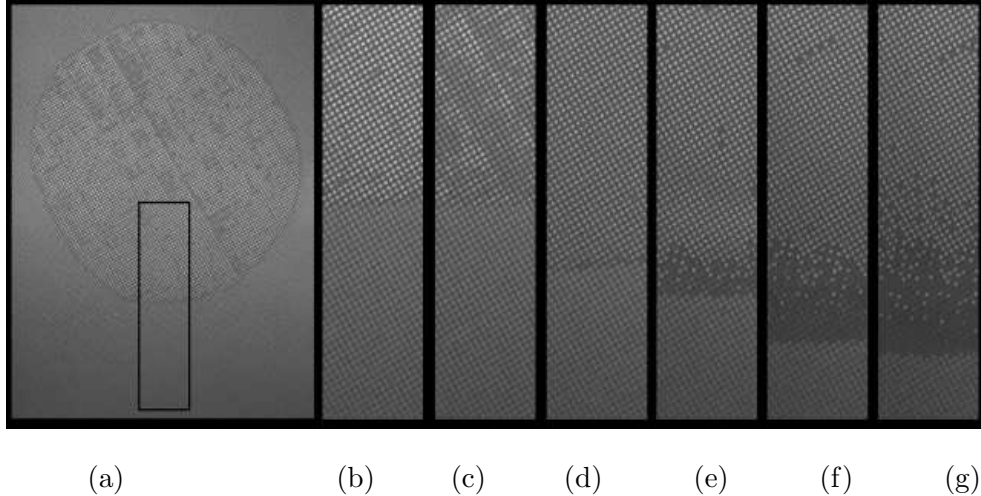


FIG. 2: View of the droplet-superhydrophobic substrate contact area. Voltage increases from left to right : (a) 0V - Cassie state, the entire contact area is shown: the droplet touches the tops of the microscopic pillars and rests on a cushion of air, (b-g) Magnified view of the black rectangle region in (a) for voltages  $U = 0 \dots 250$  (50V steps), taken during a 10 second voltage ramp. Around  $U_c \approx 150\text{V}$  the first micro-pits go to the Wenzel state (see also Fig.5).

absence of other indicators is qualitatively associated with the Wenzel state. Typically, when air is the ambient fluid, the transition is irreversible, although external intervention [4] can return the system back to the Cassie state. Irreversibility is attributed mainly to the lower energy of the Wenzel configuration and/or contact angle hysteresis. When experiments are performed in an oil environment[6], the reversibility is achieved simply by removing the applied voltage. It has been speculated that it may be due to the presence of residual oil under the droplet while in Wenzel state. A common aspect of previous EW studies is that they only provide a *macroscopic* description of the transition. We believe that access to the microscale is the key to solving problems such as the transition threshold, the dynamics of the droplet-surface liquid invasion, and ultimately, physical understanding of the irreversibility puzzle. Using this approach outside of the electrowetting context, a recent study [10] showed that, when the wetting transition is spontaneous, the Wenzel state (lower-energy) is first nucleated at a single interior point from which a wetted area expands radially. The viscous dissipation and roughness are important for determining the shape of the Wenzel wetting fronts. It is unclear if this picture is valid in the presence of electric fields.

In this paper we investigate experimentally the morphology of the Cassie-Wenzel EW-

induced transition by focusing on the droplet-substrate contact area by using reflection microscopy. In this manner, we can infer the shape of the microscopic water-air menisci formed between the microstructures during the EW-transition. To control the transition itself, the voltage applied between a drop of conductive liquid and a insulator-covered superhydrophobic surface is gradually increased, leading to an increased affinity between the drop and the substrate.

The experimental setup (Fig. 1) follows the classic EW configuration [11]: a millimeter-sized water drop sits on a ITO covered glass wafer on which a dielectric layer is applied, with the difference that here the dielectric has a micro-patterned structure. To obtain it, the wafer is first spin-coated with a SU-8[15] layer of uniform thickness  $h = 5\mu\text{m}$ . Using micro-lithography a periodic pattern of cylindrical micro-posts arranged in a square pattern (Fig. 1) is developed from an additional  $h = 5\mu\text{m}$  spin-coated SU-8 layer. The solid fraction  $\phi$  of this geometry is  $\phi = 0.196$  and the roughness (total pattern area/normal projection area) is  $r = 1.785$ . The entire structure is made hydrophobic by slowly dip-coating from a 6% Teflon AF (Dupont) solution diluted  $10\times$  in FC75. Electron microscope pictures (Fig. 1b) show that this coating does not significantly change the original geometry of the microscopic pillars. The use of this construction method ensures that the substrates remain transparent, such that we can observe the water droplet-substrate contact region from below using an inverted microscope in reflection mode. The sample was illuminated with collimated green light  $\lambda = 520\text{nm}$  and the system is in ambient air. A platinum electrode connects the water drop to a AC voltage source ( $U_{max}$  300V, frequency  $f = 5 \dots 10\text{kHz}$ ) and the electrical circuit is closed through the conducting ITO substrate.

On flat SU-8 surfaces, the Teflon AF coating provides a Young angle of  $\theta_{Y_{air}} \approx 120^\circ$ . For a micro-patterned substrate with a fraction of  $\phi$  of the surface in liquid-solid contact, the macroscopic contact angle of the Cassie-Baxter state is  $\cos \theta_{CB} = \phi \cdot \cos \theta_Y - 1 + \phi$  which is in agreement with our measurements (for  $\phi = 0.196$  the measured angle is  $\theta_{CB}^m \approx 144^\circ$ , while the theoretical one is  $\theta_{CB}^t \approx 149^\circ$ ). When an AC voltage (5kHz) is applied and slowly increased, the droplet-substrate circular contact area is observed to increase (droplet spreads). The intensity of the light reflected from individual air-liquid interfaces between the micro-pillars passes through minima and maxima, indicating that air is gradually being replaced from below the droplet. As the voltage reaches a critical value  $U > U_c \approx 150\text{V}$ , we observe at the *periphery* of the droplet-substrate contact area (Figs. 2(d) and 5) that

water invades a single ring of microscopic pits. This ring automatically forces a volume of ambient fluid to be entrapped below. This discrepancy with the random-point nucleation observed in spontaneous wetting [10] is explained by the fact that at the droplet apparent contact line the electric fields are enhanced. A quick estimate follows from the Appendix of [12]:  $E = E_a + U/\sqrt{\pi h_e \rho}$ , where the curvature  $\rho \sim h_e$ . Here  $h_e$  is the effective thickness of the equivalent capacitor below the drop, *i.e.* the edge electric fields are  $\approx \sqrt{\pi}$  higher than the average interior ones. Above  $U_c$  the droplet continues to spread and the newly covered surface is in the Wenzel state; additionally, interior micro-pits are also invaded. The trapped air becomes increasingly compressed and makes the process inefficient. (see Fig.2(e-g)). The entrapped ambient responds dynamically for experiments with fast voltage ramps ( $\ll 1$  second) or when an ambient fluid with larger viscosity (*e.g.* silicon oil) is used. Then we observed partial wetting patterns (Fig.5) that point to a dynamic instability, probably similar in origin to those observed on smooth substrates [13]. Note that the transition observed here for slow voltage ramps ( $T > 1$  second) is “smooth” : we do not observe a clear jump in the macroscopic contact angle (Fig.2(d-g) and droplet volume is conserved). This is not surprising given the one-by-one invasion process we observe.

For a quantitative relation between  $U_c$  and the individual micro-menisci shapes, we recorded the variation of the reflected light intensity coming from individual microscopic pits during the application of a linear voltage ramp to  $U > U_c$  (Fig.4. The interference curves are a measure of the (average) deviation  $d$  of the micro-menisci from flat interfaces (resting atop the pillars) under the effect of local Maxwell stresses. There are two possibilities: (1) the menisci are curved downward (Fig.1(3a, 3b) but don't advance to invade the pits unless the voltage exceeds  $U_c$  and (2) the menisci stay relatively flat and gradually fill the pits for  $U > 0$ , such that when  $U = U_c$  the pits are completely filled (Fig.1(3c)). This second scenario is eliminated by the small number of interference peaks seen before the transition (indicates  $d \ll h$  at the transition) and reversibility, *i.e.* when a voltage below  $U_c$  is removed, the light intensity returns to approximately the  $U = 0$  value).

We provide here a simple model to estimate the local contact angle at the micro-pillars for which the transition occurs. For simplicity we consider that the electric fields  $E_a$  are uniform inside the air pockets and the corresponding Maxwell stresses [14] cause a uniform curvature of the micro-menisci. The two pressures are related by the Laplace relation:  $p_{el} = \frac{\epsilon_0 E_a^2}{2} \approx \frac{\gamma}{r}$ . For a meniscus radius of curvature  $r$ , the local contact angle is given by  $\sin(\theta) = -d/(2r)$

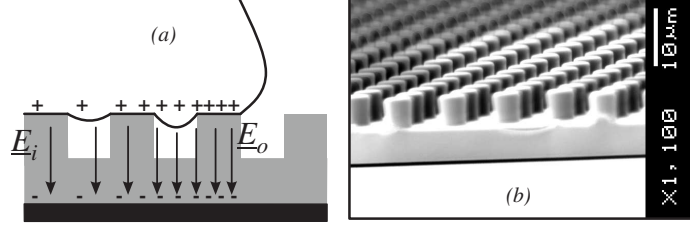


FIG. 3: (a) Micromenisci situated close to the apparent droplet contact line have higher curvature than the interior ones, as a consequence of the edge electric field enhancement:  $E_i > E_o$ .

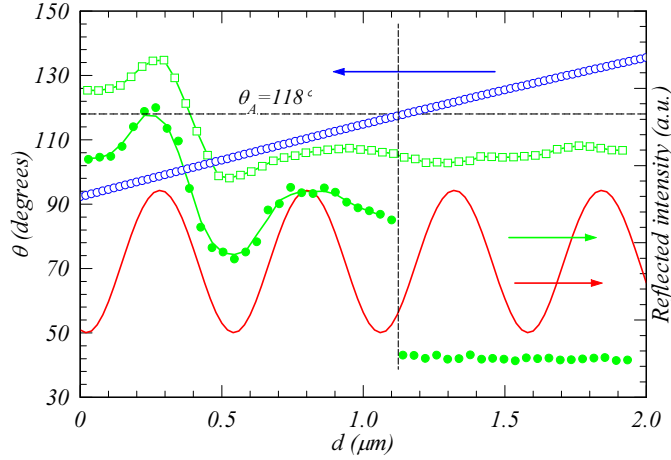


FIG. 4: Measured light intensity reflected from two selected micro-pits ( $\bullet$ ) as a function of voltage  $U$  and comparison with the calculated values for an air pocket of uniformly decreasing thickness (solid line). The sudden drop in intensity corresponds indicates the abrupt filling (Wenzel transition). For a neighboring pit ( $\bullet$  shifted vertically), the entrapped air prevents the transition. The transition is observed when the deflection  $d$  from a flat micro-meniscus is  $d \approx 1.1\mu\text{m}$ , which translates to a contact angle  $\theta \approx 118^\circ$  ( $\circ$  curve).

and the maximum deviation from pillar tips is  $d = r(1 - \sin(\pi - \theta))$ . We will approximate the height of the air pockets at a given voltage  $U$  to be simply  $h - d$ , where  $h$  is the depth of the micro-pits (Fig.1(3b)).

For a uniformly decreasing height of the air-pockets starting from  $h$ , the calculated change in the reflected line intensity is shown in Fig.4(b). As we are only interested in the behavior of  $d$  with  $U$  and not in the exact functional dependence. This is then compared to two curves from Fig4(b) from the interior region, one that will fill (filled symbol) and one stable (open symbol). We rescaled the positions of the two measured interference maxima so that

they coincide with the calculated ones. Then we can simply “read out” the  $h - d$  value for the transition and translate it into a curvature using the arguments given earlier. The contact angle for the transition, corresponding to the sudden drop in the measured intensity is then  $\theta_m \approx 118^\circ$ , which is of the order of the advancing contact angle of a triple water-air-Teflon AF interface on a smooth substrate. Why is the rest of the interior air pockets not filling simultaneously? As some of the air pockets are filled, the droplet contact line is “sealed” and we expect the pressure in the neighboring ones to increase slightly and delay the filling of other pits to higher applied voltages. The larger the water-impregnated area, the more stable the remaining air-pockets become, which should be the reason for not observing the full-transition at the highest voltages we applied ( $> 300\text{V}$ ). The other possibility is, obviously, the saturation effect[11]. We have noticed that for improperly coated micro-patterned substrates the transition occurs at a significantly smaller voltage premature and the inferred critical contact angle for the transition is close to that of the bare SU-8 surface ( $\approx 94^\circ$ ).

In spite of the robustness of the dielectric, the electrowetting effect saturated before we could squeeze a significant fraction of the interior micro-pits to fill up; we have observed that for the highest voltages, as the trapped air is confined to smaller regions, it forms shallow bubbles which may rise above the pillar structure. When the voltage is applied very fast (the extreme case corresponds to a voltage step), we see organized patches of similar sizes (Fig.5) of impregnated micro-pits rather than isolated single ones (“quasi-static” case). Additional experiments performed in silicone oil (Fluka AS4 with viscosity  $\mu \approx 6\text{mPa}\cdot\text{s}$ ) produced similar results for slower voltage ramps.

To summarize, we have performed the first microscale study of the morphology and dynamics of the EW-induced wetting transition of a droplet on a superhydrophobic surface. We have identified that the transition always originates at the apparent droplet-patterned substrate contact line, due to locally higher fringe electric fields. The impregnation of the micro-structure with liquid is only partial due to the entrapping of a finite volume of air below the electrowetting drop. This situation is aggravated at high rates of increasing voltage, when dynamic wetting patterns are observed. Their formation can be slowed down if an oil is used instead of air as ambient liquid. In order for a micro-pit to be filled with water, the curvature caused by the local maxwell stresses has to be sufficiently high such that the local contact angles exceed the advancing value in the absence of electric fields.

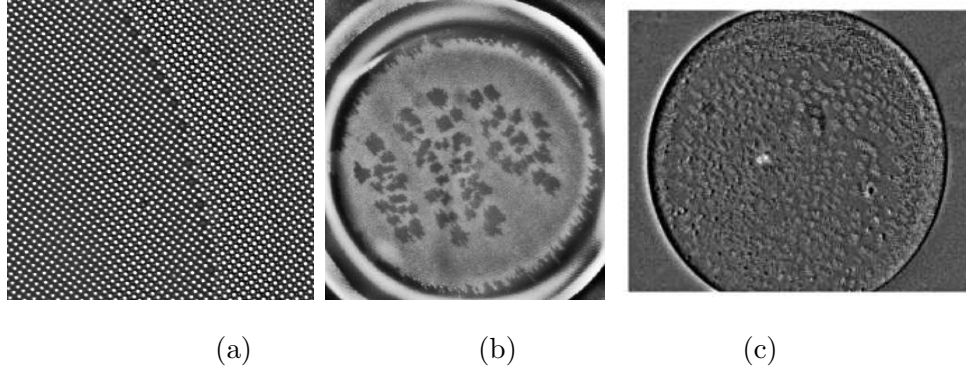


FIG. 5: (a) Incipient state of the EW-induced wetting transition: due to increased electric fields at the contact line (3), a single ring of air-pockets collapses first. (b) Partial Wenzel state wetting pattern obtained after the application of fast voltage ramps. The dynamics of the process is essentially the same, but slowed down considerably, when the experiment is performed in silicon oil environment (c). Imaging oil-water interfaces is however more difficult due to smaller refractive index contrast.

We believe that this is essentially a nucleated thin-film dewetting of ambient fluid, initially trapped between the droplet and the substrate.

Financial support within the joint program Micro- and Nanofluidics by the MESA+ institute for nanotechnology and by the IMPACT institute at Twente University is gratefully acknowledged.

---

\* Electronic address: a.d.staicu@tnw.utwente.nl

- [1] D. Quéré, Reports on Progress in Physics **68**, 2495 (2005).
- [2] R. Wenzel, Industrial & Engineering Chemistry **28**, 988 (1936).
- [3] A. Cassie and S. Baxter, Trans. Faraday Soc **40**, 546 (1944).
- [4] T. Krupenkin, J. Taylor, T. Schneider, and S. Yang, Langmuir **20**, 3824 (2004).
- [5] D. Herbertson, C. Evans, N. Shirtcliffe, G. McHale, and M. Newton, Sensors and actuators. A, Physical **130**, 189 (2006).
- [6] M. Dhindsa, N. Smith, J. Heikenfeld, P. Rack, J. Fowlkes, M. Doktycz, A. Melechko, and M. Simpson, Langmuir **22**, 9030 (2006).
- [7] N. Verplanck, E. Galopin, J. Camart, V. Thomy, Y. Coffinier, and R. Boukherroub, Nano

- Lett **7**, 813 (2007).
- [8] Z. Wang, Y. Ou, T. Lu, and N. Koratkar, *J. Phys. Chem. B* **111**, 4296 (2007).
  - [9] L. Zhu, J. Xu, Y. Xiu, Y. Sun, D. Hess, and C. Wong, *Journal of physical chemistry. B, Condensed matter, materials, surfaces, interfaces, & biophysical chemistry* **110**, 15945 (2006).
  - [10] M. Sbragaglia, A. Peters, C. Pirat, B. Borkent, R. Lammertink, M. Wessling, and D. Lohse, *Phys. Rev. Lett.* **99**, 156001 (2007).
  - [11] F. Mugele and J. Baret, *J. Phys.: Condens. Matter* **17**, 705 (2005).
  - [12] M. Vallet, M. Vallade, and B. Berge, *Europ. Phys. J. B* **11**, 583 (1999).
  - [13] A. Staicu and F. Mugele, *Phys. Rev. Lett.* **97**, 167801 (2006).
  - [14] F. Mugele and J. Buehrle, *Journal of Physics: Condensed Matter* **19**, 375112 (2007).
  - [15] standard polymeric photo-resist used in micro-lithography